Experimental investigation of multi-effect regenerator for desiccant dehumidifier: Effects of various regeneration temperatures and solution flow rates on system performances

Datta, Nirmalya; Chakraborty, Anutosh; Ali, Syed Muztuza; Choo, Fook Hoong

2017

Datta, N., Chakraborty, A., Ali, S. M., & Choo, F. H. (2017). Experimental investigation of multi-effect regenerator for desiccant dehumidifier: Effects of various regeneration temperatures and solution flow rates on system performances. International Journal of Refrigeration, 76, 7-18.

https://hdl.handle.net/10356/86278

https://doi.org/10.1016/j.ijrefrig.2017.01.019

Experimental Investigation of Multi-effect Regenerator for Desiccant Dehumidifier: Effects of Various Regeneration Temperatures and Solution Flow rates on System Performances

Nirmalya Datta[1], Anutosh Chakraborty[2,*], Syed Muztuza Ali[2], F.H. Choo[3]

[1]Interdisciplinary Graduate School, Nanyang technological University

[2]School of Mechanical and Aerospace Engineering, Nanyang Technological University

50 Nanyang Avenue, Singapore 639798, Republic of Singapore

[3]Energy Research Institute @ NTU, Nanyang Technological University, CleanTech One,

Singapore 637141, Republic of Singapore

[*]Corresponding Author: AChakraborty@ntu.edu.sg, Tel: +65-67904222

Abstract

We have experimentally measured the thermal performances (PR) of vacuum assisted multi-effect regenerator, which employs hydrophobic membrane to separate water vapor from LiCl solution with higher evaporation rates. We have modified the working principles of the conventional multi-effect membrane distillation (MEMD) by the transfer of heat from one stage to the other stage of regenerating module such that more energy can be recovered through multi-effect evaporation generated in each regenerating module with enhanced liquid vapor separation in the membrane. The PR and percentage change in desiccant concentration are measured for the temperatures ranging from 50 ^{o}C to 75 ^{o}C. The experimental results show that the conventional MEMD is not suitable for dehumidification applications due to higher feed concentration. We have modified the conventional MEMD system employing (i) one-steam-three-solution passes and (ii) two-steam-four-solution passes, which handles higher feed concentrations. The PR is found 0.7 for one steam three solution passes system.

Keywords: Multi-effect-regenerator, desiccant dehumidifier, low temperature heat, performance ratio, concentrations

1. Introduction

The energy consumption of buildings has been increased significantly due to population growth and economic development. As the air-conditioning (AC) systems make up 50% of energy consumption by buildings, there should be energy efficient AC systems with acceptable indoor air quality (IAQ) [1–3]. Conventional heating ventilation and air-conditioning (HVAC) systems play a major role in commercial as well as residential buildings sector. The major drawback to the AC system is that it does not have the capability to meet latent and sensible loads independently at reasonable energy consumptions. Conventionally, the humidity is reduced by cooling air below the dew point temperature of the space, causing moisture to condense on the cooling coil. The air is then heated to a designed temperature before being discharged into the space. This means that the process of sensibly over cooling and then heating air requires unnecessary consumption of energy. Therefore, a highly energy efficient air-conditioning system is required.

The liquid desiccant technologies are gained much emphasis over the past decade, especially in the tropical countries due to high relative humidity (RH) of air. Liquid desiccants, which include halide salt solutions, have a strong affinity with moisture to dehumidify air streams. This is due to the fact that desiccants have an equilibrium vapor pressure that is lower than the vapor pressure of air, and this vapor pressure difference creates a driving potential for moisture transfer. As a result, the amount of water vapor in the salt solution increases. Energy is consumed to heat up the liquid desiccants to a temperature where the pressure of liquid desiccant is greater than air so that moisture can be released [4, 5]. The regeneration process can be accomplished with low quality energy sources such as waste or solar heat [6]. It should be noted here that the major drawback to direct contact liquid desiccant systems is the carry-over of

desiccant solution aerosols into the airstream. The desiccant solutions are corrosive in nature which corrodes the air ducts whenever it comes in contact with metallic surfaces and hence affects the longevity of the system [7, 8]. The addition of polymeric hydrophobic membranes has gained much attention in liquid desiccant air-conditioning (LDAC) system as the membranes ensure zero carry-over of desiccant-solution-aerosols in the air stream, thereby eliminating the drawbacks of air contamination and corrosion of direct desiccant-air contact systems [9, 10]. In addition, the LDAC system has also the ability of utilizing liquid desiccants to store the latent heat of condensation during the regeneration process [11].

The LDAC is not a new concept [12]. There has been continuous development in this field since its advent in the 1930s. During the 1930s and 40s, Alexis Berestneff started working on LiBr-H_2O systems for the Carrier Corporation, and at the same decade his contemporary Edmund Altenkirch and Francis Bichowsky were developing concepts and technical solutions for open absorption systems [13]. The LDAC system utilizes the semi-permeable membrane for both air dehumidification (air moisture is absorbed on the salt solution) and solution regeneration processes (moisture is removed from the salt solution). Up to now, two types of membrane technologies are gained attention in LDAC research. One is the LAMEE (liquid-air-membrane heat exchanger) for HVAC applications [14] and the other is RAMEE (run-around-membrane heat exchanger) for passive energy recovery in buildings [15]. These membranes provide high surface area for interaction between the fluids resulting in high heat and mass transfer rates across the membrane. It should also be noted here that the PTFE (Poly tetra-fluoro ethylene) hydrophobic membranes are microporous flat sheet type with good gas permeability, and can be used for LDAC research [16]. The LDAC system mainly comprises absorption bed, regenerator and a cooling cycle. In this paper, we mainly focus on the experimental investigation of

desiccant regenerator, which is a multi-stage vacuum graded multi-effect-membrane-distillation (V-MEMD) system especially designed for desalination purposes [17]. This V-MEMD technology amalgamates the advantages of multi-effect-evaporation and vacuum for highly efficient heat recovery as compared with conventional dehumidification processes [18-22]. The solar or any waste heat driven heater is used to drive the V-MEMD module. The membrane distillation mechanism is shown in Figure 1. It is observed that water molecules are separated from the salt solution due to pressure difference between the feed solution and the water vapour. The temperature and pressure gradients are occurred by direct permeation through membrane pores, which provides fast water vapour transport with hydrophobic effects. Vacuum is always applied to the permeate side of the membrane. The vapour pressure and temperature gradually decreases from steam riser to the condenser. The multi-effect design reduces the overall thermal energy consumption during regeneration process and also utilizes the merits of both the multi-effect distillation and the mass transfer across the membrane separating the solution from the distillate. The recent development and perspective of membrane distillation [23-29] are highlighted in Table 1. However, our research targets are to apply V-MEMD module to remove water vapor from the liquid desiccant salt solution for the dehumidification of AC purposes. Hence, we have modified the working principles of conventional V-MEMD [17, 30, 31].

The main aim of this manuscript is to reduce energy consumption by the use of membrane based multistage regenerator, which possesses an acceptable performance ratio (PR) at the heat source temperatures ranging from 50 to 73 ^{o}C. The objectives are the experimental investigation of V-MEMD as the generator of LDAC system to analyze the effects of various operating parameters on change in concentration (ΔC) as well as the thermal performance ratio (PR). The ΔC and PR of (i) single stage steam-three stages desiccant (1S-3L), (ii) two stages steam-three stages

desiccant (2S-2L) and (iii) conventional V-MEMD distillation are investigated experimentally under various feed flow rates, feed concentrations and heating temperatures.

2. Experiments

Materials

The absorption modules, steam riser and the condenser modules are made from synthetic material to avoid the high corrosiveness of the liquid desiccant salt solution. For the membrane modules, hydrophobic PTFE membrane laminate (functional layer: PTFE, back material: Polypropylene) with a reference pore size of 0.2 μm, and 0.12 ~ 0.2 mm thickness are used for the separation process. The desiccant salt used for the feed solution in this experimental test and evaluation was LiCl with a mass concentration (mass fraction) of 8% to 36%. The scanning electron micrograph (SEM) images of rear side reinforced PTFE and front side PP hydrophobic membrane layers are shown in Figures 2(a) and 2(b), respectively.

Concentration of LiCl salt solution

Lithium Chloride LiCl anhydrous with a minimum purity of 99.9% is used in this work. Dry mass of the sample is required to calculate the concentration, C of aqueous solution (mass fraction in terms of mass of salt per mass of solution). Before measuring the dry mass of LiCl salt, the samples are heated up to 90 °C and kept 4 hours under vacuum condition by a vacuum oven to make sure that there is no moisture in the samples. The distilled water is used as the solvent in all aqueous solutions. PRECISA micro balance, with ±0.0001 g accuracy, was applied to measure the mass of solvent and solutes (dry salts). The concentration parameter is calculated from the known mass of solute and solution. The density of aqueous solution at known concentration is measured by means of Anton Paar DMA 5000M (Vibrating tube density meter;

accuracy density: 0.000005 g cm^{-3}) at various temperature points (accuracy Temperature: 0.01 °C/0.02 °F). The LiCl salt solution data are also available in Literature [32].

Experimental setup

The complete experimental setup consists of two sub-systems (i) absorber or liquid-to-air membrane heat exchanger, in which the liquid absorbent circulates and absorbs moisture from the moist air and (ii) regenerator or multi-effect-membrane distillation, in which a thermally driven process allows water vapor (generated from the weak liquid desiccant solution) transport through hydrophobic porous membranes. The scheme diagram of the test bed is shown in Figure 3. It consists of three working cycles namely the absorption cycle, the regeneration cycle and the cooling cycle. The absorption-regeneration system comprises hydrophobic membrane assisted dehumidifier (as shown ABS in the schematic), a hydrophobic membrane based regenerator (depicted as REG in the schematic) and intermediate storage tanks for concentrated and dilute lithium chloride solutions (depicted as $TANK_1$ and $TANK_2$), respectively. The storage tanks are made of Polypropylene (PP), and it can handle intermittent temperatures up to 95 °C and are resistant to the corrosive nature of lithium chloride. Both tanks are provided with PP nozzles for the transportation of the LiCl solution. A heat exchanger (HEX) is employed for heat exchange between the dilute and the concentrated absorbent solutions. Two centrifugal /reciprocating pumps are used in this absorbent circuit, one is located at the exit of the regenerator and the other is at the exit of the concentrated tank. The butterfly valves are used to control the flow rate of lithium chloride solution at the entry and the exit of the absorber. The butterfly valves are also used to control the flow rate of cold water at inlet and exit of the absorber.

The cooling cycle employs R134a refrigerant and produces cooling effects at the evaporator by transferring heat from the low to the high temperature regions through the compression and expansion of refrigerant. In the evaporator, the heat exchange is occurred between the chilled

water and the refrigerant. The chilled water is then circulated through the cooling coils by a pump. The function of the installed pumps is to maintain a steady volumetric flow rate of the fluids in the system. The dehumidified air extracted from the absorber (ABS) is cooled in the duct by the cooling coils. The air ducts carry conditioned air into the room and are fitted with air dampers. The function of the dampers is to control the flow of the air, or can even prevent the air from entering specified areas. By regulating air flow, the duct damper can be used to control temperature and humidity levels and also restrict the flow of dangerous fumes or smoke. The power consumption of air dampers of the test bed is 2 V while running and 1 V while holding. The regeneration unit as also shown in Figure 3 performs the regeneration of water vapor from the dilute desiccant solution arriving from the absorber via dilute storage tank. The regenerator comprises multiple stages, and each stage consists of six poly-propylene (PP) plastic foil frames and five poly tetra-fluoro ethylene (PTFE) membrane frames. The modules are welded alternately with space between the foil frame and the membrane frame. This space provides the channel for a uniform flow of the desiccant solution for the regeneration of each stage. The concentrated desiccant at the exit of the regenerator is pumped back to the concentrated desiccant tank from where it is again used for dehumidification in the absorber.

Working principles of LDAC regenerator

Vacuum multi-effect-membrane-distillation (V-MEMD) system amalgamates the advantages of multi-effect evaporation and the merit of the membrane's mass transfer process. Since this product is designed for the desalination and water treatment industry, it works very well when the feed concentration is as low as sea water concentration (% Concentration in mass is less than 10%) [17]. However, the minimum operation concentration of the regeneration process for liquid desiccant air-conditioning (LDAC) system is 26%. According to the preliminary test, a conventional 4 stages V-MEMD system [31], which is shown in Figure 4 (a), fails to provide

satisfactory performance above 22% feed concentration. Therefore, for dehumidification purposes, the conventional 4 stage V-MEMD system should be modified. For operating the LDAC with high feed concentration (26 ~ 40%), the following configurations can be proposed:

(i). Hybrid 1S-3L V-MEMD system (steam in single stage and liquid desiccant flows in three stages). The schematic diagram is shown in Figure 4(b).

(ii). Hybrid 2S-4L V-MEMD system (steam is two stages and liquid desiccant flows in four stages). The schematic diagram is shown in Figure 4(c).

The key components of the multi-effect regenerator are steam riser, regenerating modules, condenser, heat exchangers and a vacuum pump. The steam riser module is made of PTFE membrane and the condenser module is constructed using PP foils. Hot water generating from the solar collector system or any auxiliary heater flows through the heat exchanger, and a pump in the secondary loop of the heat exchanger circulates the hot water in the steam riser. Due to the temperature and pressure gradient across the membrane, the frames operate under a vacuum environment, water vapour is produced and the generated steam crosses the PTFE membrane where it is channelled to the foil modules of the 1st stage of the regenerator. The steam is condensed by the cooler feed solution flowing on the other side of the foil. In this regenerator, the condensate from the first stage is circulated back to the heat exchanger to top up the water loss due to the condensation. The temperature of the feed solution rises by capturing the latent heat of condensation at the foil. The temperature and pressure gradient across the membrane causes the steam to flow through the membrane and the steam is then channelled to the next stage. The vaporization causes the diluted feed into strong or concentrated solution and the concentrated solution is channelled to the next stage. In the next stage, the steam generated from the membrane frame of first stage flows into the foil frame of second stage, condensing into steam and at same time, the latent heat of condensation is recovered by the concentrated feed

solution of the first stage. Finally, the steam generated from the fourth stage of the regenerator unit goes into the foil frames of the condenser. In this last stage, all the remaining steam is condensed. The pictorial view of the regenerator system is shown in Figure 5. The dimensions of each regenerator module are height, 70 cm × width, 70 cm × thickness (gap), 15 cm.

Performance parameters

The parameters that influence the performances of the proposed desiccant regenerator for dehumidification purposes are feed desiccant (here LiCl) concentration, feed flow rates and the driving heat source temperatures. In this experiment (i) the feeding concentrations are ranged from 8 % to 36 %, (ii) the feeding flow rates are varied from 0.15 litre/min to 1 litre/min, (iii) the hot water temperatures are set at 50, 55, 65 and 75 ^{o}C with the cooling water inlet temperature of 28 ^{o}C. The change in concentration ΔC (in %) is calculated by $\Delta C = C_i - C_o$, where C_i and C_o indicate the concentrations of aqueous lithium chloride solution at inlet and exit of the regenerator. In this manuscript, the performance of the multistage generator is calculated in terms of performance ratio (PR). The thermal performance ratio in terms of kW per kW can be expressed as the ratio of the heat generation for distillation process (water vapor separation from the salt solution) to the average heating energy. The PR is written as

$$PR = (m_{dist} \times h_{fg})/H_{in}, \quad (1)$$

where $m_{dist} = \rho_{sol}. V_{sol}. (C_o - C_i)/C_o$. H_{in} (kW) is the heat energy input to the system and is calculated by the hot water flow rate, and the temperature difference between the hot water flowing into and out of the steam riser.

Instrumentation and measurements

The pressure sensors are installed at various points of the system for measuring the pressure at inlet and outlet of the absorber. Special pressure sensors (uncertainty, ±2% of measurement scale) are installed at the inlet and the outlet line of the solution, which are resilient to corrosion by the absorbent. A Coriolis flow meter (error ±0.5% of the full scale) is installed to measure the mass flow rate of the desiccant solution at the inlet of the absorber. The pressure is also measured at air inlet and air exit of the absorber. The velocity meter is used for measuring the velocity of air entering the absorber. The relative humidity is measured at the inlet and outlet of air channel using relative humidity sensors. Volumetric flow meters are used to measure the volumetric flow rates at the cooling and heating water outlets. All data are recorded by a Schneider Electric data logger for further analysis. Hence, the experimental testing was conducted at least three times to check the repeatability of the experimental data. Employing the uncertainty analysis, the errors of PR are calculated and the errors are ranged from 1% to 8% depending on LiCl solution flow rates.

3. Results and discussion

An experimental investigation was carried out to measure the performances of LDAC regenerator employing LiCl desiccant solution. In this experiment, the feed concentration ranges from 8% to 22% and the feed flow rates are varied from 0.15 litre/min to 1 litre/min. The thermal performances as functions of heating source temperatures and solution flow rates are plotted in Figures 6(a), 6(b) and 6(c) for the inlet salt concentrations of 8%, 15% and 22%. These results show that at 8% feed concentration (similar to sea water), the performance ratio (PR) varies from 2 to 2.5. These PR values are comparable with those of the conventional multi-effect evaporator for desalination purposes [17]. However, for the higher concentration of 22%, the PR value drops sharply from around 2 to 0.65 (Figure 6c) with the regeneration temperature of 80 ^{o}C. For

lower concentrations and feed flow rates, the concentration difference between inlet and outlet (ΔC) is large due to the recovery of more heat. The change in ΔC of the regenerator module for various solution flow rates and regeneration temperatures are shown in Figures 7(a), 7(b) and 7(c) at inlet feed concentrations of 8%, 15% and 22%. At higher feed concentrations and flow rates, the Δ*C* is found smaller. The sharp decrease in PR at higher concentrations can be attributed to the vapour pressure characteristics of aqueous LiCl solutions. The vapour pressure of liquid desiccants is inversely related to the desiccant concentration. As the concentration increases, the vapour pressure drops. Therefore, the amount water vapour from liquid desiccant decreases and the PR drops. On the other hand, the driving heat source temperature plays a significant role on the increase in PR of LDAC regenerator. This is due to the fact that the vapour pressure is directly related to the temperature of desiccant solution, and at higher heating temperatures, the solution absorbs more heat with the increase of vapour pressure, which in turn increases its ability to lose more water. It should also be noted here that the overall heat transfer coefficient decreases due to the lower thermal conductivity at higher feed concentration. The PR increases with increase in flow rates of the feed solution. The study shows that the conventional 4-stage V-MEMD system [17, 31] performs very well under the regeneration temperature of 50 $^{\circ}$C with 8% feed concentration. However, at higher concentration (22% or higher), the overall performance drops drastically. Therefore, the conventional 4 stage V-MEMD is not suitable for dehumidification purposes. Hence, the performance ratios of the proposed one-steam-three-solution (1S3L) and two-steam-four-solution (2S4L) stages are presented.

The functions of steam riser and condenser of the proposed 1S3L and 2S4L are same as those of conventional V-MEMD regenerator system. Only the configurations of steam and solution stages are modified to improve the performance of regenerator system for higher salt concentrations.

The solution with feed concentration of 27%, 32%, 34% and 38% are applied at different feed flow rates and different hot water temperature in the steam riser. The temperature charts of 1S3L system are shown in Figure 8. Due to energy utilization and heat losses to the ambient, the temperature of steam at stage 3 is lower than that at stage 1. The test results related to change in concentration (ΔC) and PR of the 1S3L regenerator system at the salt concentration level of 27%, 30% and 32% for the hot water temperature of 55 ^{o} C with feed flow rates ranging from 0.17 to 1 litre/min are shown in Figures 9 (a) and 9(b). It is found that the PR increases with the increase in feed flow rates. At 27% inlet feed concentration and the solution flow rate of 0.17 litre min^{-1}, the ΔC shows the highest value and decreases gradually with the increase in feed flow rates up to 1 litre min^{-1}, due to insufficient heat to remove the moisture from salt. Here the change in concentration is varied from 5% to 2%. However, at the inlet feed concentration of 32%, ΔC is increased, which is nearly constant at about 0.8%. The maximum performance ratio is achieved 0.6 at 27% salt concentration and 0.83 litre min^{-1} feed flow rate. At higher concentrations, the performance ratio drops significantly. Figures 10(a) and 10(b) show the variations of ΔC and PR at 65 ^{o}C for the feed concentrations of 27%, 30%, 34%, and 38%, where the feed flow rates are varied from 0.15 litre min^{-1} to 1 litre min^{-1}. It is found that the change in ΔC drops with the feed flow rate. The highest ΔC are found 9%, 4%, and 3% for the inlet feed concentration of 27%, 34%, and 38% at the solution flow rate of 0.17 litre min^{-1}. At feed flow rate of 1 litre min^{-1}, the values of ΔC are measured to be 3%, 2.2%, and 2% (Figure 10a). The maximum PRs are calculated as 0.65, 0.45, and 0.35 at 27%, 34%, and 38% inlet feed concentration for the solution flow rates of 0.83 litre min^{-1}, 0.67 litre min^{-1} and 0.67 litre min^{-1}, respectively. All these results are furnished in Figure 10(b). Figures 11(a) and 11(b) show the concentration increase and performance ratio at 31%, 34% and 38% feed concentration with the hot water temperature of 75 ^{o}C. At the feed concentration of 31%, the maximum and minimum increases in concentrations

are 6.7% and 3.2% for feed flow rate of 0.17 litre min^{-1} and 0.76 litre min^{-1}, respectively. The maximum performance ratio is achieved as 0.4 at the feed flow rate of 0.55 litre min^{-1}. At the feed concentration of 38%, the highest and lowest ΔC are calculated to be 4% and 1% for feed flow rates of 0.17 litre min^{-1} and 1 litre min^{-1}. The maximum PR is calculated to be 0.28 for the feed low rate of 0.56 litre min^{-1}.

The functions of steam riser and condenser as well as the desiccant materials are same as those of 1S3L regenerator system. Hence, the configurations of steam and solution stages are modified (Figure 3c) to improve the performances of regenerator system. The temperature variations as a function of time at 32% concentration for the proposed 2S4L system are shown is Figure 12. Here, the concentration of 32% at different feed flow rates and different hot water temperatures in steam riser (60 ^{o}C, 75 ^{o}C, and 85 ^{o}C) are employed. The results for ΔC and PR of 2S4L system at the feed concentration of 32% are shown in Figures 13(a) and 13(b). With the increase in hot water temperature, the % ΔC increases and shows nearly the same values at different feed flow rates (Figure 13a). As can be seen from Figure 13(b), the highest performance ratio is achieved 0.5 for the solution flow rate of 0.83 litre min^{-1}.

For all cases, the ΔC is found greater at higher heating temperatures, and this is due to the temperature difference between the hot water and the feed desiccant solution separated by the polymer foil which may provide a greater driving force for the removal of water vapor from the feed solution across the membrane. Figures 9(a), 10(a), 11(a) and 13(a) also reveal that the increase in concentration (ΔC) is significantly lower for higher inlet concentrations (C_i) even at higher heating temperatures and decreases even more at a higher feed flow rate. At higher inlet concentrations, the solution provides higher resistance to the removal of water vapor from the

solution due to its higher vapor pressure. It is observed from the test results that the PR increases with the increase in temperature for both the low and high concentration feed solution. This occurs due to the fact that the higher heating temperature increases the pressure difference and as a result the vapour pressure of the salt solution in a partial vacuum condition increases the water vapour separation rate from the liquid desiccant, which also enhances the thermal performance ratio. It should also be noted here that the resident time of the salt solution in the membrane module is lessened due to its higher flow rates, and the proper desorption of water vapour from the salt solution is not achieved. Therefore the reduction in ΔC and PR can be obtained.

At higher concentrations (>29%) feed inlet, the value of ΔC is low for lower feed velocity. Therefore, an optimum feed flow rate exists for maximizing the concentration increment and PR, which can be attributed to the requirement of an optimum residence period for the feed solution to utilize the latent heat of vaporization essential for effective regeneration. In 1S3L system operation, the performance ratio is not significantly improved with the increase in heating water temperature for the feed concentrations higher than 30%, which may be occurred due to heat loss from the regenerating module. It is hoped that the 2S 4L system should be the most efficient system amongst all the three configurations. But experimentally, this system produced poor performance due to design restriction. More research activities and experimental studies are needed to improve this configuration. Therefore, 1S3L system is considered as efficient design for dehumidification purposes.

4. Conclusions

In this paper, the thermal performances (in terms of kW distillation per kW heat input) of 4-stage V-MEMD are calculated for various inlet feed concentrations ranging from 8% to 22% and flow

rates up to 1 litre/min. The PR is obtained 2.5 for the heating water temperature of 50 ^{o}C with the inlet feed concentration of 8%, which is suitable for desalination applications. The PR increases at higher feed inlet temperature. However, at higher feed concentrations, the PR decreases significantly. At 22% feed concentration, the PR drops up to 0.65 with the heat source temperature of 80 ^{o}C. For desiccant dehumidification conditions (concentration > 22%), the PR drops drastically with the heating water temperature of 65 ^{o}C and the system does not perform even with the source temperature of 55 ^{o}C. The conventional V-MEMD is not suitable for desiccant dehumidification. The working principles of the regenerating module are modified with the combinations of steam and LiCl solution flows in each module such that the system can handle high concentration feed for dehumidification applications. The first configuration deals with steam flows in single stage and liquid desiccant flows in three stages where the low grade energy is recovered. The PR is found to be 0.7 for the heating temperature of 55 ^{o}C with 27% inlet feed concentration. This configuration also works well for the feed concentration of 32% at 55 ^{o}C. At the higher heating temperature of 75 ^{o}C, the PR drops due to heat loss from the system. The second configuration is based on steam flows in two stages and liquid desiccant flows in four stages for better heat recovery at the fourth stage. The fourth sage is designed with the supply of re-generated steam from LiCl solution. As can be observed from experimental data, this system provides poor performance ratio even at higher temperature. It may be occurred due to more heat losses in the last stage at higher temperature. From the present analysis, it is concluded that V-MEMD module, which is generally designed for desalination purposes, can also be employed for desiccant regeneration applications.

Acknowledgements

The authors would like to thank Energy Research Institute (ERI@N), Singapore for supporting the experimental testbed facility. Mr. Nirmalya acknowledges Interdisciplinary Graduate Studies (IGS), NTU for the Research Scholarship and ERI@N for continuous support throughout the research. The authors also acknowledge the financial supports from A* Star, MND and Building Construction Authority (BCA), Singapore (Project No. SERC 112 176 0024).

Nomenclature

PR	Thermal Performance Ratio
ΔC	The change in concentration between the inlet and outlet of the single stage generator [%]
C_i	Concentration of feed at inlet [%]
C_o	Concentration of feed at outlet [%]
m_{dist}	Mass flow rate of distillate [kg. s^{-1}]
H_{in}	Heat Input [kW]
h_{fg}	Heat of vaporization [kJ. kg^{-1}]

References

1. D. Kolokotsa, D. Rovas, E. Kosmatopoulos, and K. Kalaitzakis, A roadmap towards intelligent net zero- and positive-energy buildings, Solar Energy, vol. 85, pp. 3067-3084, Dec 2011.

2. D.P.Wyon, The effects of indoor air quality on performance and productivity, Indoor Air, Vol. 14, pp. 92-101, 2004.

3. A. M. Omer, Energy, environment an sustainable development, Renew.Sustain.Energy Rev. Vol. 12, pp. 2265-2300, 2008.

4. M. R. Conde, Properties of aqueous solutions of lithium and calcium chlorides: formulations for use in air conditioning equipment design, International Journal of Thermal Sciences, Vol. 43, pp. 367-382, 2004.

5. Z. Y. Xu, R. Z. Wang, H. B. Wang, Experimental evaluation of a variable effect LiBr-water absorption chiller designed for high-efficient solar cooling system, International Journal of Refrigeration, Vol. 59, pp. 135 – 143, 2015.

6. J. Wang, J. Wu, H. Wang, Experimental investigation of a dual-source powered absorption chiller based on gas engine waste heat and solar thermal energy, Energy, Vol. 88, pp. 680 – 689, 2015.

7. Y. Chen, X. Zhang, Y. Yin, Experimental and theoretical analysis of liquid desiccant dehumidification process based on an advanced hybrid air-conditioning system, Applied Thermal Engineering, Vol. 98, pp. 387 – 399, 2016.

8. S. Yamaguchi, S., J. Jeong, K. Saito, H. Miyauchi, M. Harada, Hybrid liquid desiccant air conditioning system: Experiments and simulations, Applied Thermal Engineering, Vol. 31, pp. 3741 – 3747, 2011.

9. L. Z. Zhang, Progress on heat and moisture recovery with membranes: From fundamentals to engineering applications, Energy Conversion and Management, Vol. 63, pp. 173 – 195, 2012.

10. L.Z. Zhang and N.Zhang, A heat pump driven and hollow fiber membrane-based liquid desiccant air dehumidification system: modelling and experimental validation, Energy, Vol. 65, pp. 441-451, 2014.

11. S. M. Pineda, G. Diaz, Performance of an adiabatic cross-flow liquid-desiccant absorber inside a refrigerated warehouse, International Journal of Refrigeration, Vol. 34, pp. 138 – 147, 2011.

12. B. G. Nimmo, Jr. R. K. Desiccant enhancement of cooling based dehumidification, ASHRAE Transaction, Vol. 99, pp. 842 – 848, 1993.

13. F. R. Bichowsky, G. A. Kelley, Concentrated Solutions in Air-conditioning, Industrial and Engineering Chemistry, Vol. 27, pp. 879 - 882, 1935.

14. M. R. H., Abdel-Salam, G. Ge, M. Fauchoux, R. W. Besant, C. J. Simonson, State-of-the-art in liquid-to-air membrane energy exchangers (LAMEEs): A comprehensive review, Renewable and Sustainable Energy Reviews, Vol. 39, pp. 700 – 728, 2014.

15. K.Mahmud, G.I.Mahmood, C.J.Simonson, and R. W. Besant, Performance testing of a counter cross flow run-around membrane energy exchanger RAMEE system for HVAC applications, Energy Build., Vol. 42, pp. 1139-1147, 2010.

16. D. Singh, K. K. Sirkar, High temperature direct contact membrane distillation based distillation using PTFE hollow fibers, Chemical Engineering Science, Vol. 116, pp. 824 – 833, 2014.

17. S. Wang, Y. Wang, Investigation of the through plane effective oxygen diffusivity in the porous media of PEM fuel cells: Effects of the pore size distribution and water saturation distribution, International Journal of heat and Mass Transfer, Vol. 98, pp. 541 – 549, 2016.

18. K.Gommed and G.Grossman, A liquid desiccant system for solar cooling and dehumidification, J. Solar Energy Engg., vol. 126, pp. 879-885, 2004.

19. K.Gommed and G.Grossman, Experimental investigation of a liquid desiccant system for solar cooling and dehumidification, Solar energy, Vol. 81, pp. 131-138, 2007.

20. Y. Yin, X. Zhang, and Z. Chen, Experimenatl study on dehumidifier and regenerator of liquid desiccant cooling air conditioning system, Building and Environment, vol. 42, pp. 2505-2511, 2007.

21. X. H. Liu, Y. Jiang, and K. Y. Qu, Heat and mass transfer model of cross flow liquid desiccant air dehumidifier/regenerator, Energy Conversion and Management, vol. 48, pp. 546-554, Feb 2007.

22. G.A. Longo and A. Gasperella, Experimental and theoretical analysis of heat and mass transfer in a packed column dehumidifier/regenerator with liquid desiccant, Int J. Heat and Mass Tranfer, vol. 48, pp. 5240-5254, 2005.

23. Kim, Y.-D., Thu, K., Ghaffour, N., Choon Ng, K., Performance investigation of a solar-assisted direct contact membrane distillation system, Journal of Membrane Science , 427, pp. 345-364, 2013.

24. Lee, J.-G., Kim, Y.-D., Kim, W.-S., Francis, L., Amy, G., Ghaffour, N., Performance modeling of direct contact membrane distillation (DCMD) seawater desalination process using a commercial composite membrane, Journal of Membrane Science, 478, pp. 85-95, 2015.

25. C.M. Guijt, G.W. Meindersma, T. Reith, A.B. de Haan, Air gap membrane distillation: 2. Model validation and hollow fibre module performance analysis, Separation and Purification Technology, Vol. 43, pp. 245–255, 2005.

26. Aryapratama, R., Koo, H., Jeong, S., Lee, S., Performance evaluation of hollow fiber air gap membrane distillation module with multiple cooling channels, Desalination, Vol. 385, pp. 58-68, 2016.

27. Mohammad Mahdi A. Shirazi , Ali Kargari & Meisam Tabatabaei, Sweeping Gas Membrane Distillation (SGMD) as an Alternative for Integration of Bioethanol Processing: Study on a Commercial Membrane and Operating Parameters, Chemical Engineering Communications, 202:457–466, 2015.

28. K. Zhao, W. Heinzl, M. Wenzel, S. Büttner, F. Bollen, G. Lange, S. Heinzl, N. Sarda, Experimental study of the memsys vacuum-multi-effect-membrane-distillation (V-MEMD) module, Desalination, Vol. 323, pp. 150–160, 2013.

29. Lian, B., Wang, Y., Le-Clech, P., Chen, V., Leslie, G., A numerical approach to module design for crossflow vacuum membrane distillation systems, Journal of Membrane Science, Vol. 510, pp. 489-496, 2016.

30. M Kumja, FH Choo, B Li, A Chakraborty, ET Mohan Dass, K Zhao, S Dubey, Two Dimensional Numerical Analysis of Membrane-based Heat and Mass Cross Flow Exchanger Heat Transfer Engineering, Article in Press, **DOI:**10.1080/01457632.2016.1195139.

31. F.H. Choo, M. KumJa, K. Zhao, A. Chakraborty, ETM Dass, M. Prabu, *et al.*, Experimental study on the performance of membrane base multi-effect dehumidifier regenerator powered by solar energy, Energy Procedia, Vol. 48, pp. 535-542, 2013.

32. P. Emmott, A concentration-cell method for the determination of trace amounts of chloride in solutions of lithium salts, The Analyst, Vol. 90, pp. 482-487, 1965.

List of Figures

Figure 8: Temperature profiles of various components of 1S3L regenerator under steady state conditions.

Figure 9: (a) Increase in concentration and (b) performance ratio (PR) against solution flow rates of one-steam-three-solution regenerator configuration for the inlet feed concentrations of 27%, 30% and 32% at 55 ^{o}C.

Figure 10: (a) Increase in concentration and (b) performance ratio (PR) against solution flow rates of one-steam-three-solution regenerator configuration for the inlet feed concentrations of 27%, 30%, 34% and 38% at 65 ^{o}C.

Figure 11: (a) Increase in concentration and (b) performance ratio (PR) against solution flow rates of one-steam-three-solution regenerator configuration for the inlet feed concentrations of 31%, 34% and 37% at 75 ^{o}C.

Figure 12: Temporal history for various components of two-steam-four-solution system for the heat sources of 60 ^{o}C and 75 ^{o}C.

Figure 13: (a) Increase in concentration and (b) performance ratio (PR) against solution flow rates of two-steam-four-solution regenerator configuration for the temperatures of 60, 75 and 80 ^{o}C at the inlet feed concentration of 32%.

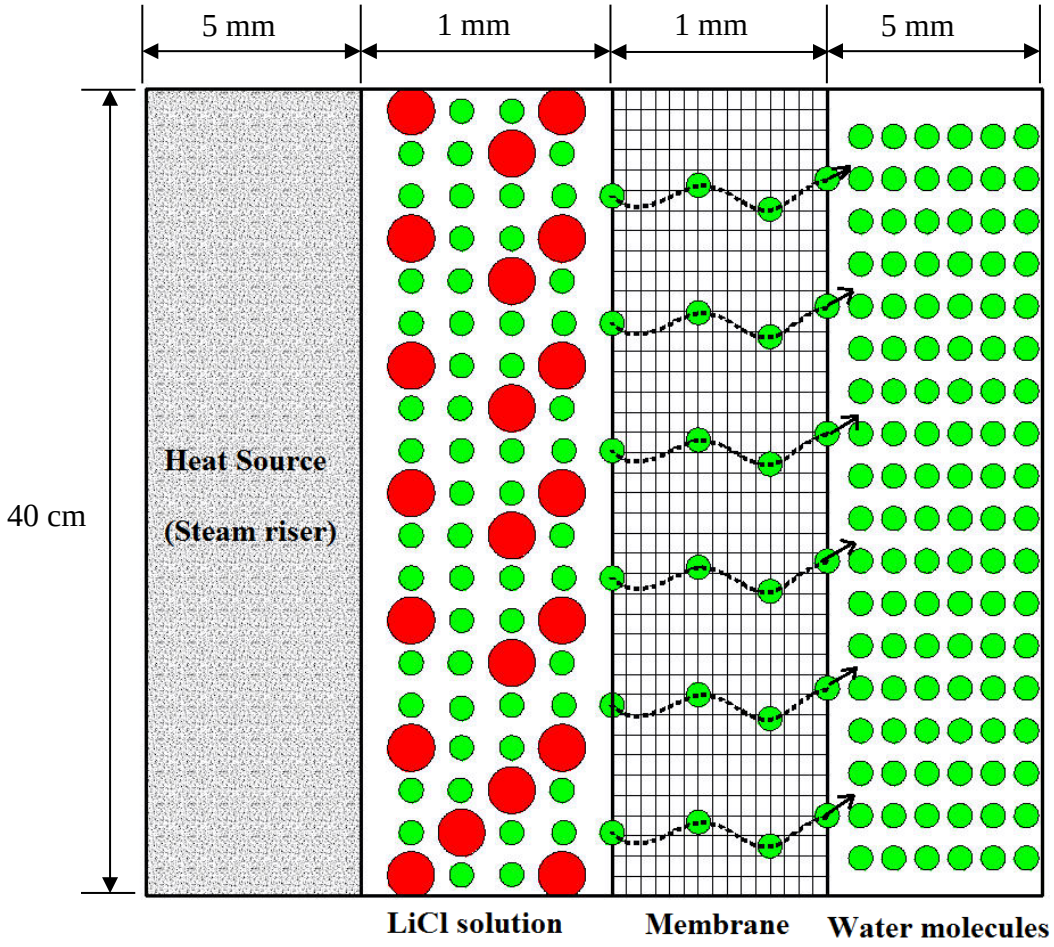
5 mm
1 mm
1 mm
5 mm
40 cm
Heat Source
(Steam riser)
LiCl solution
Membrane
Water molecules

Figure 1

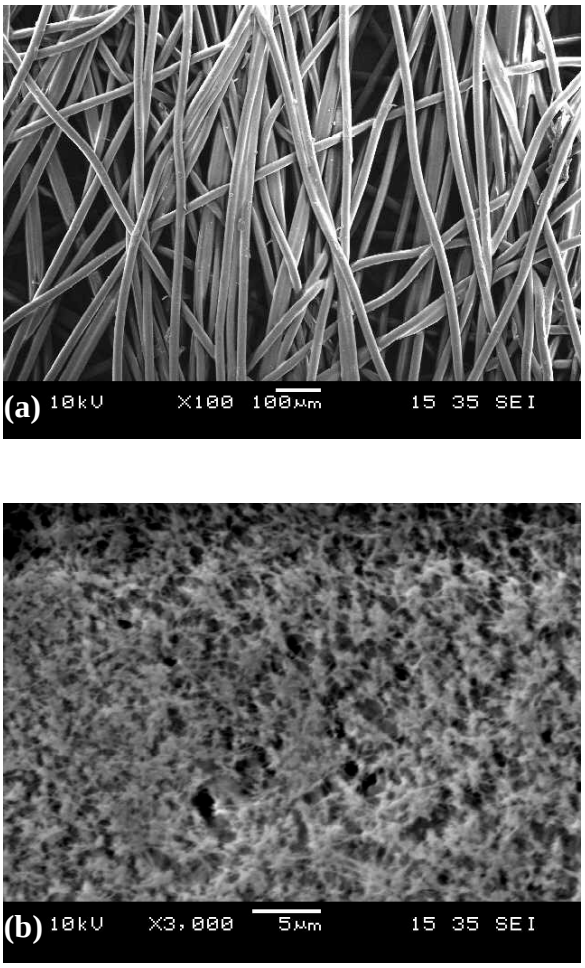

Figure 2

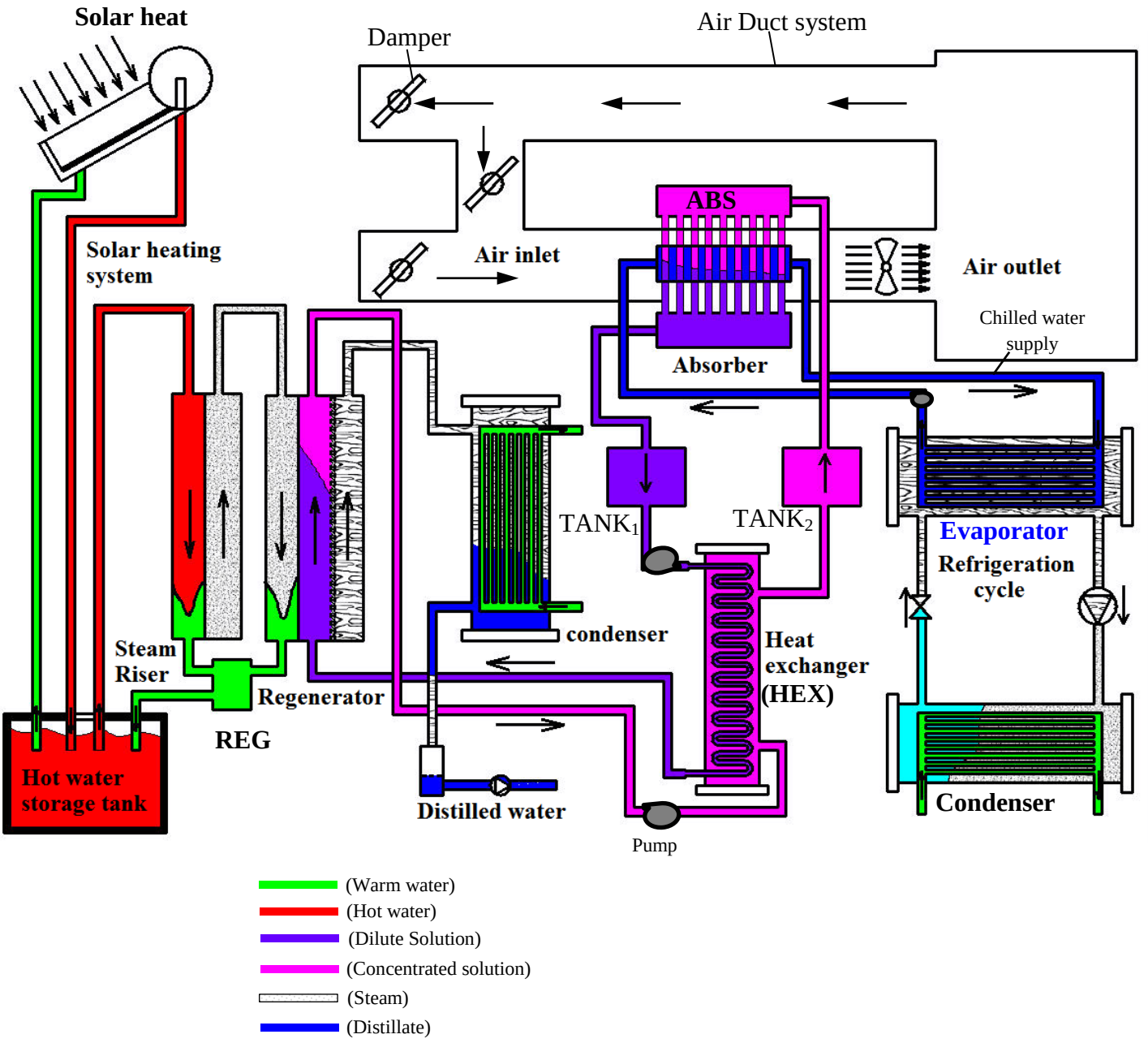
Solar heat
Damper
Air Duct system
ABS
Air inlet
Air outlet
Solar heating system
Chilled water supply
Absorber
TANK1
TANK2
Evaporator
Refrigeration cycle
condenser
Heat exchanger (HEX)
Steam Riser
Regenerator
REG
Hot water storage tank
Distilled water
Pump
Condenser
(Warm water)
(Hot water)
(Dilute Solution)
(Concentrated solution)
(Steam)
(Distillate)

Figure 3

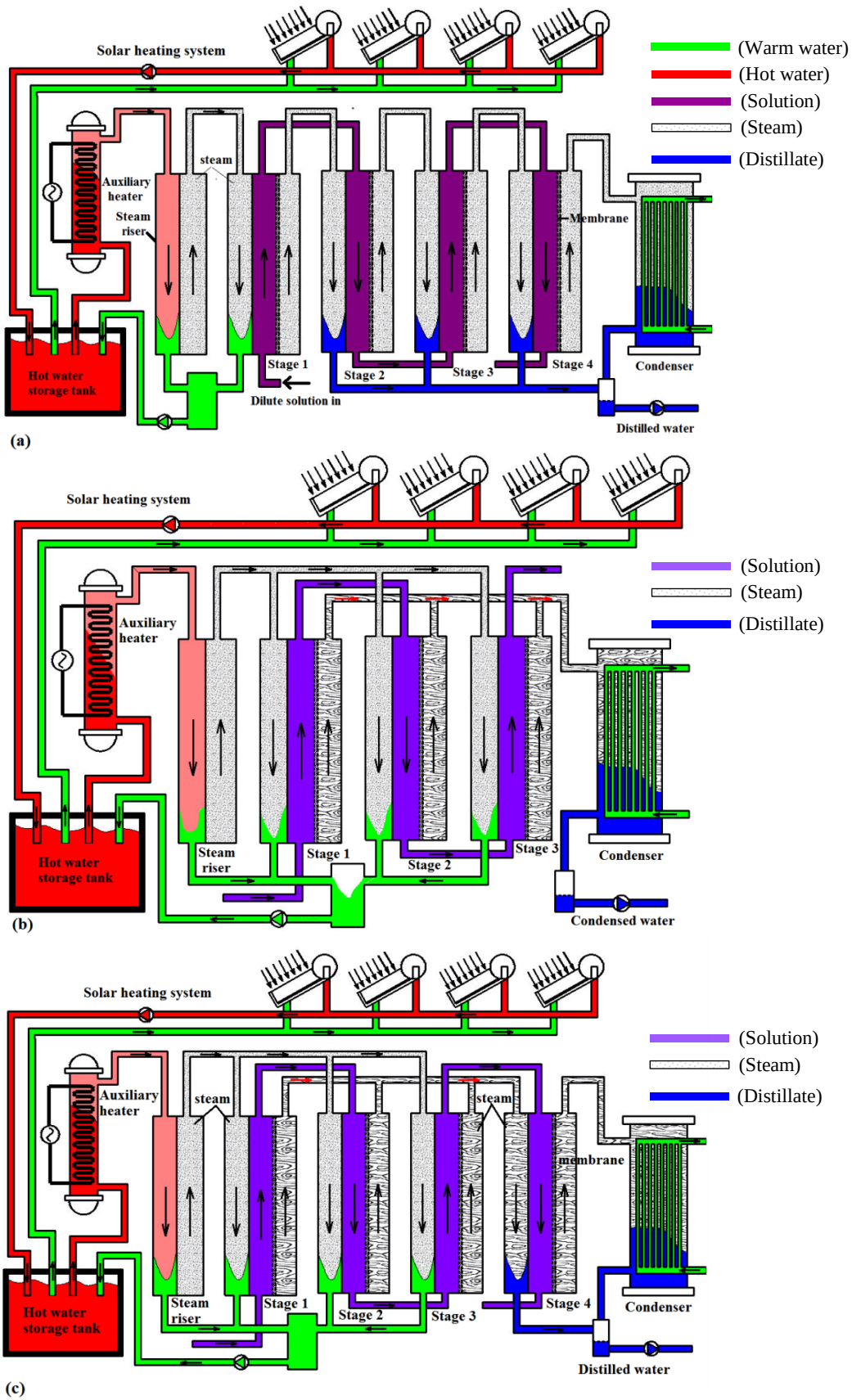
Solar heat
Solar heating system
(Warm water)
(Hot water)
(Solution)
(Steam)
(Distillate)
steam
Auxiliary heater
Steam riser
Membrane
Hot water storage tank
Stage 1
Stage 2
Stage 3
Stage 4
Condenser
Dilute solution in
Distilled water
(a)
Solar heating system
(Solution)
(Steam)
(Distillate)
Auxiliary heater
Steam riser
Stage 1
Stage 2
Stage 3
Condenser
Hot water storage tank
Condensed water
(b)
Solar heating system
(Solution)
(Steam)
(Distillate)
Auxiliary heater
steam
steam
membrane
Steam riser
Stage 1
Stage 2
Stage 3
Stage 4
Condenser
Hot water storage tank
Distilled water
(c)

Figure 4

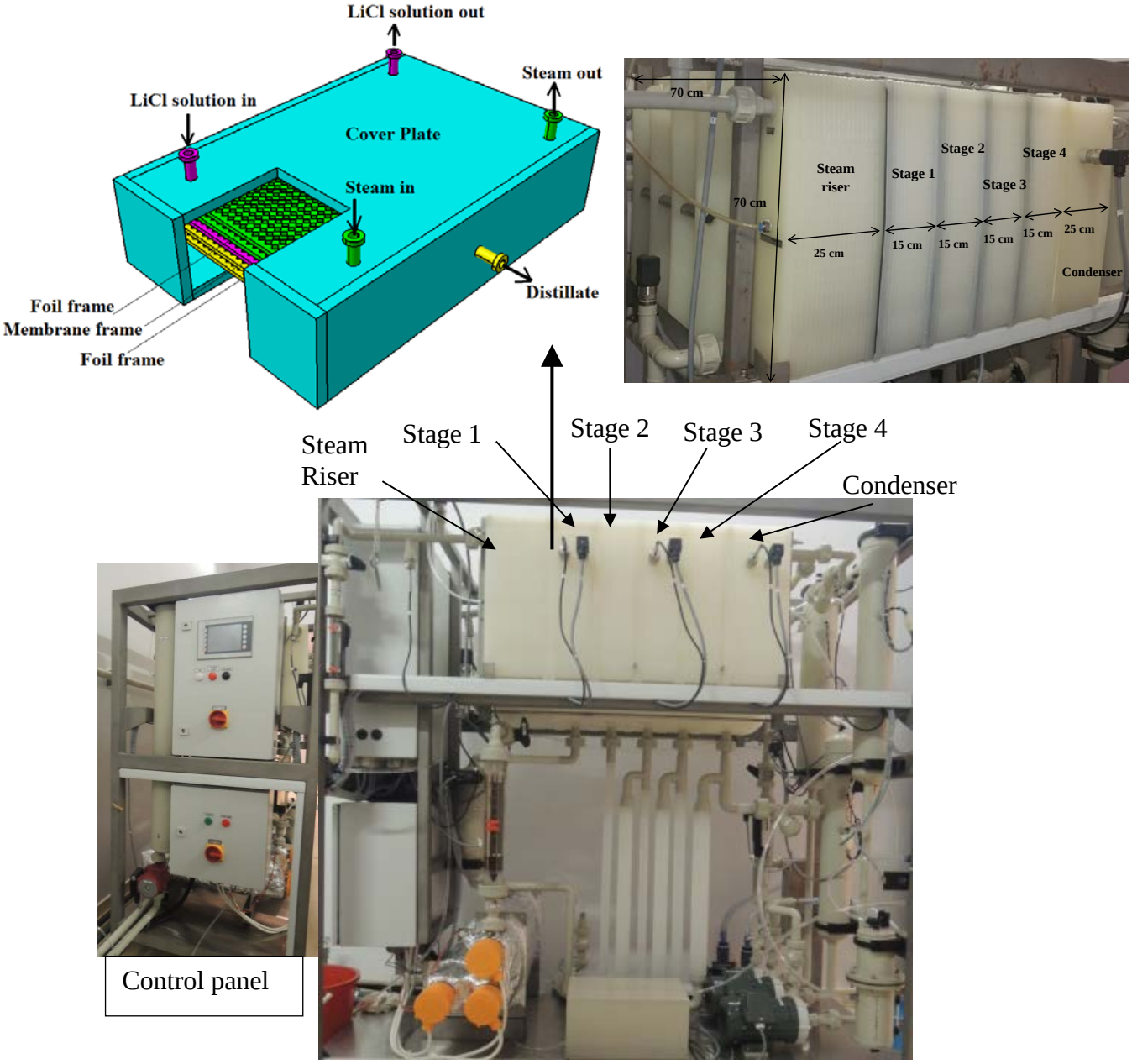
LiCl solution out
LiCl solution in
Steam out
Cover Plate
Steam in
Distillate
Foil frame
Membrane frame
Foil frame
70 cm
70 cm
Steam riser
Stage 1
Stage 2
Stage 3
Stage 4
25 cm
15 cm
15 cm
15 cm
15 cm
25 cm
Condenser
Steam Riser
Stage 1
Stage 2
Stage 3
Stage 4
Condenser
Control panel

Figure 5

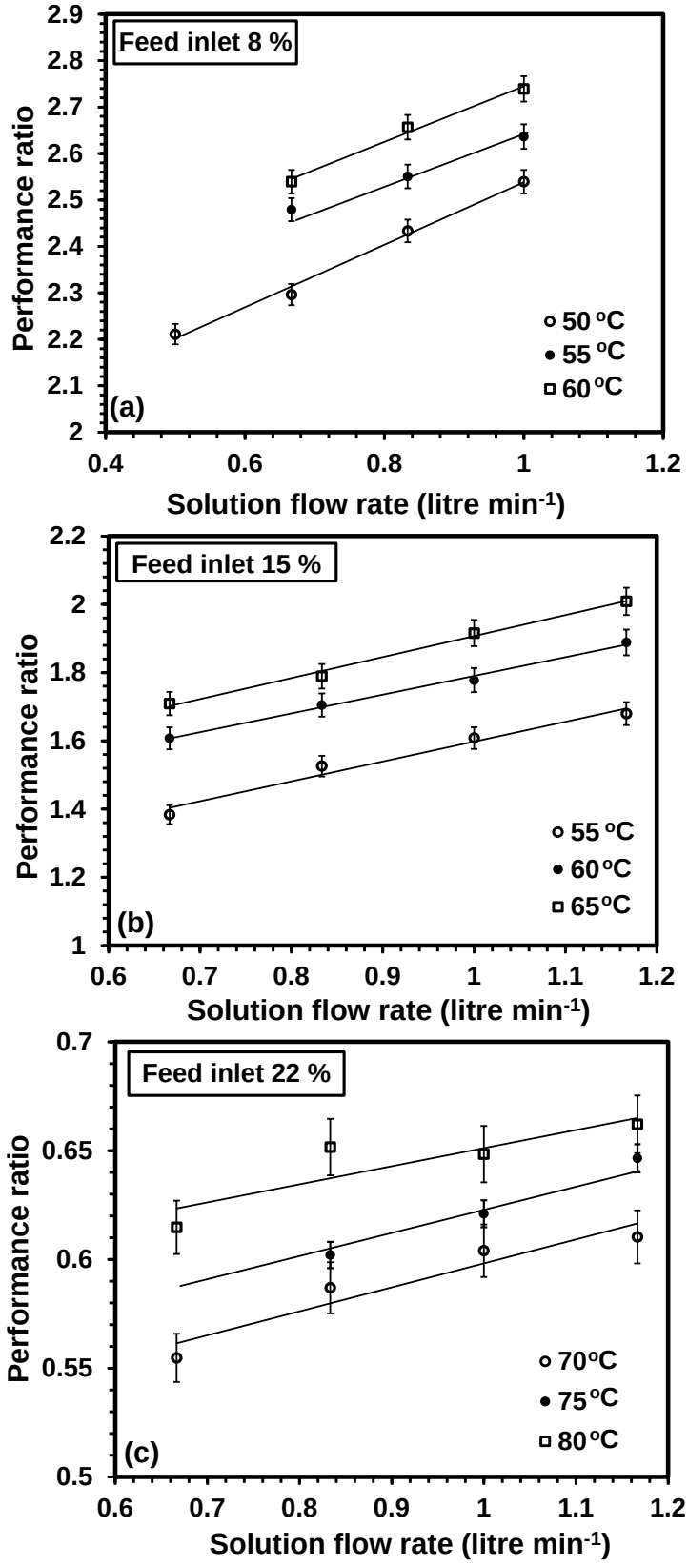
Feed inlet 8 %
Performance ratio
Solution flow rate (litre min-1)
50 °C
55 °C
60 °C
(a)
Feed inlet 15 %
Performance ratio
Solution flow rate (litre min-1)
55 °C
60 °C
65 °C
(b)
Feed inlet 22 %
Performance ratio
Solution flow rate (litre min-1)
70 °C
75 °C
80 °C
(c)

Figure 6

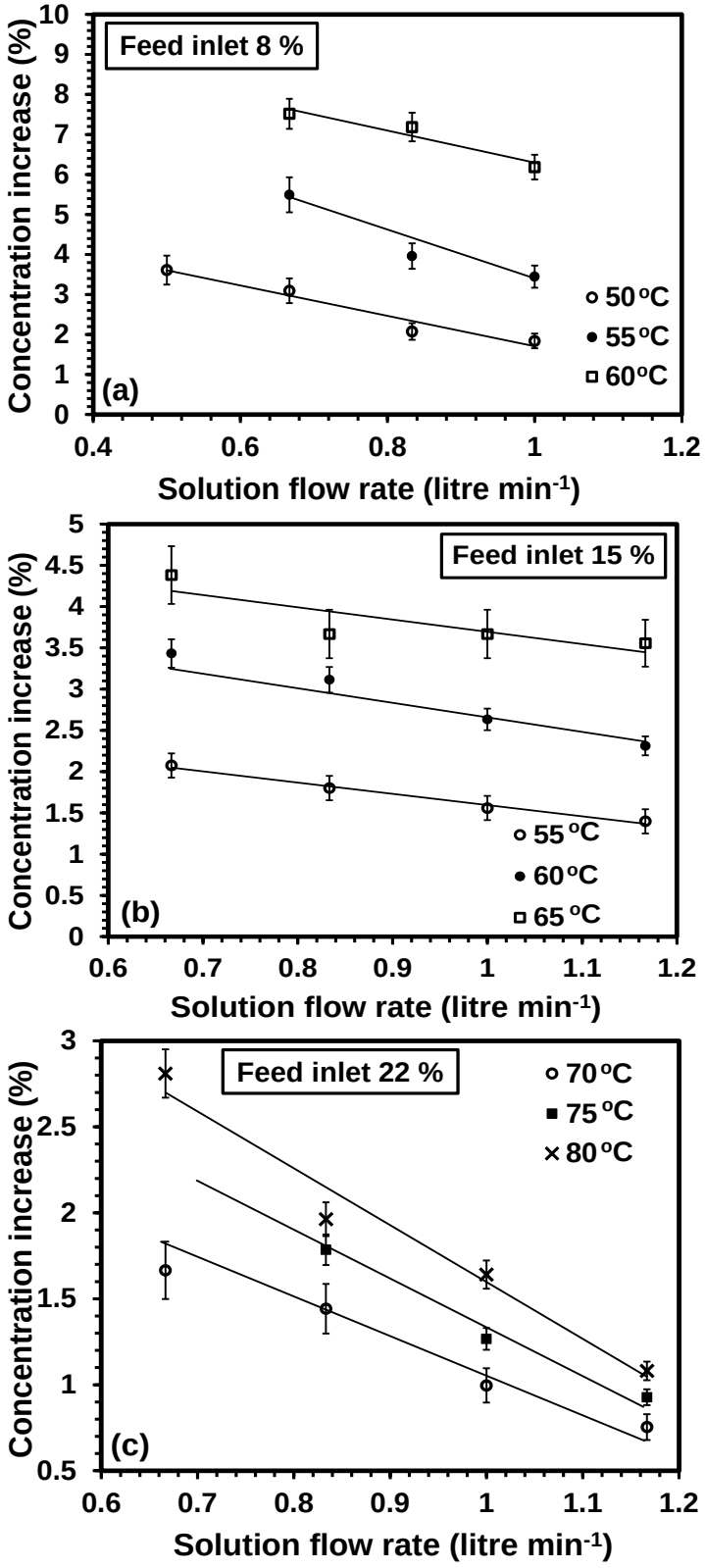
Feed inlet 8 %
Concentration increase (%)
Solution flow rate (litre min-1)
50 °C
55 °C
60 °C
(a)
Feed inlet 15 %
55 °C
60 °C
65 °C
(b)
Feed inlet 22 %
70 °C
75 °C
80 °C
(c)

Figure 7

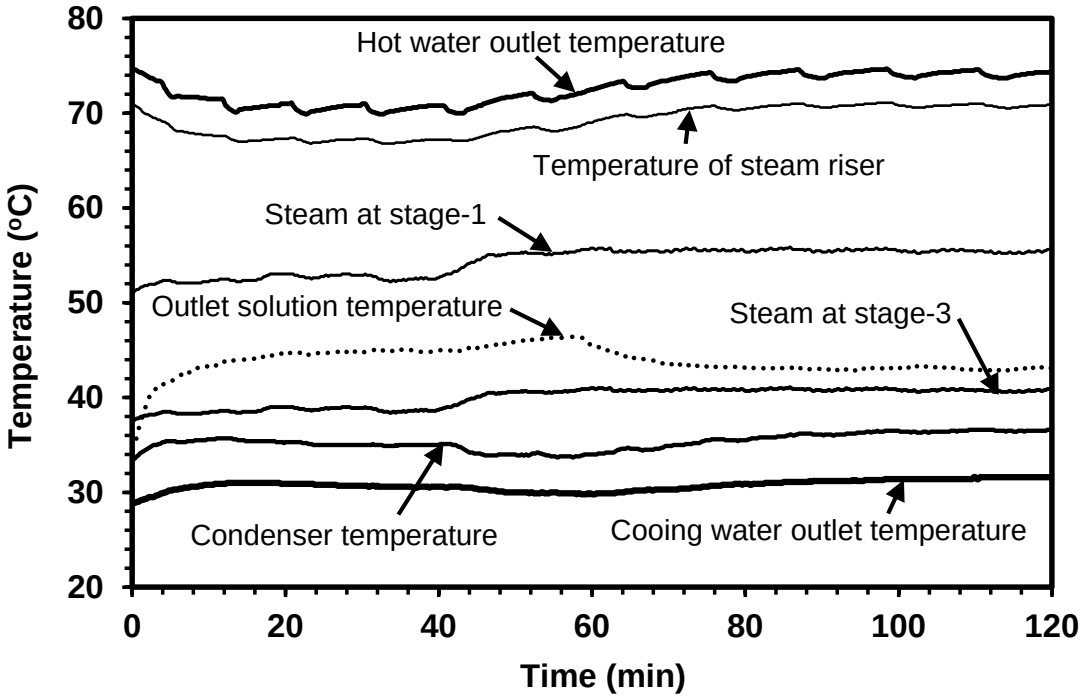
Hot water outlet temperature
Temperature of steam riser
Steam at stage-1
Outlet solution temperature
Steam at stage-3
Condenser temperature
Cooing water outlet temperature
Temperature (°C)
Time (min)
80
70
60
50
40
30
20
0
20
40
60
80
100
120

Figure 8

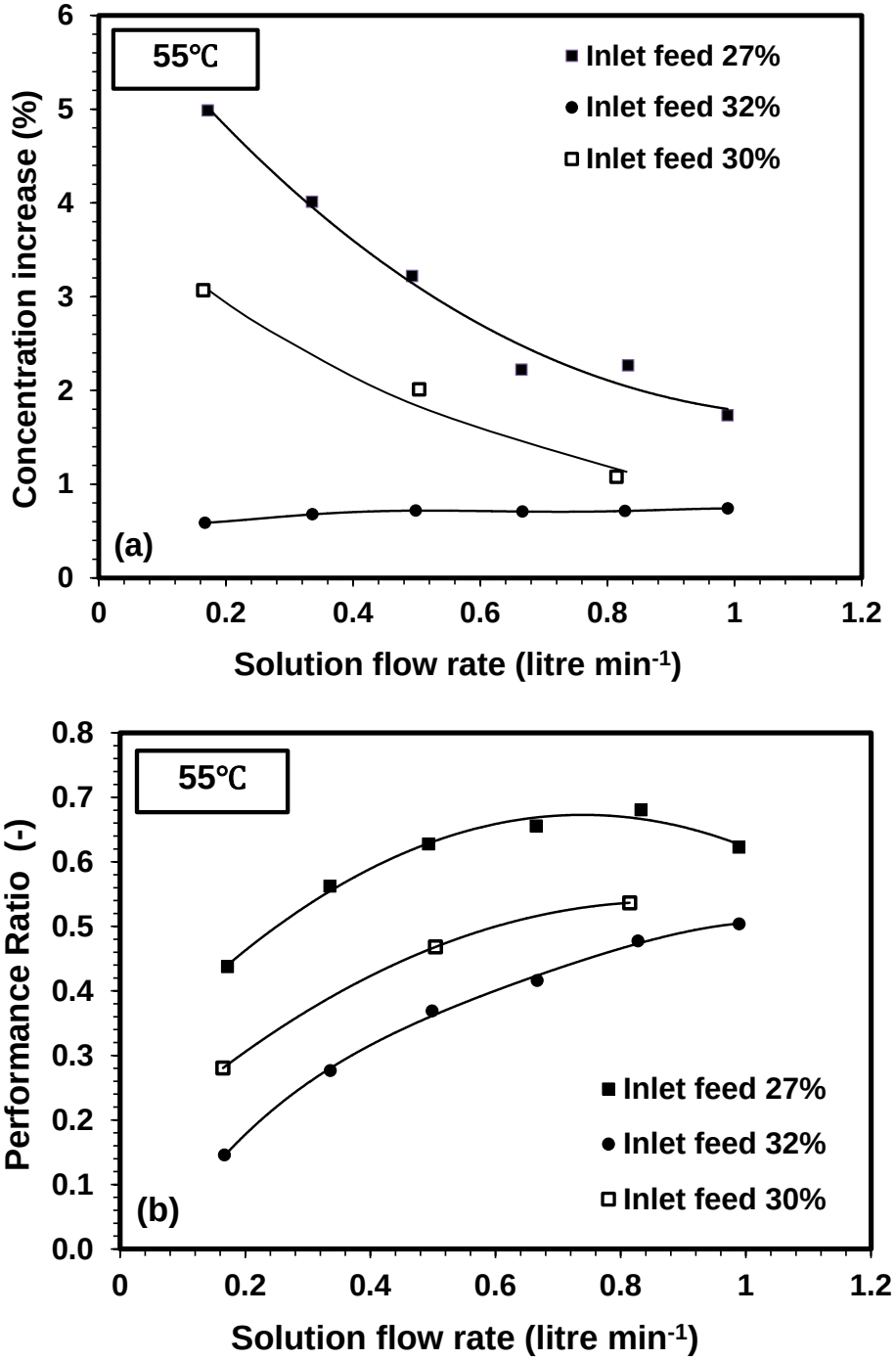
55℃
Inlet feed 27%
Inlet feed 32%
Inlet feed 30%
Concentration increase (%)
(a)
Solution flow rate (litre min-1)
55℃
Performance Ratio (-)
Inlet feed 27%
Inlet feed 32%
Inlet feed 30%
(b)
Solution flow rate (litre min-1)

Figure 9

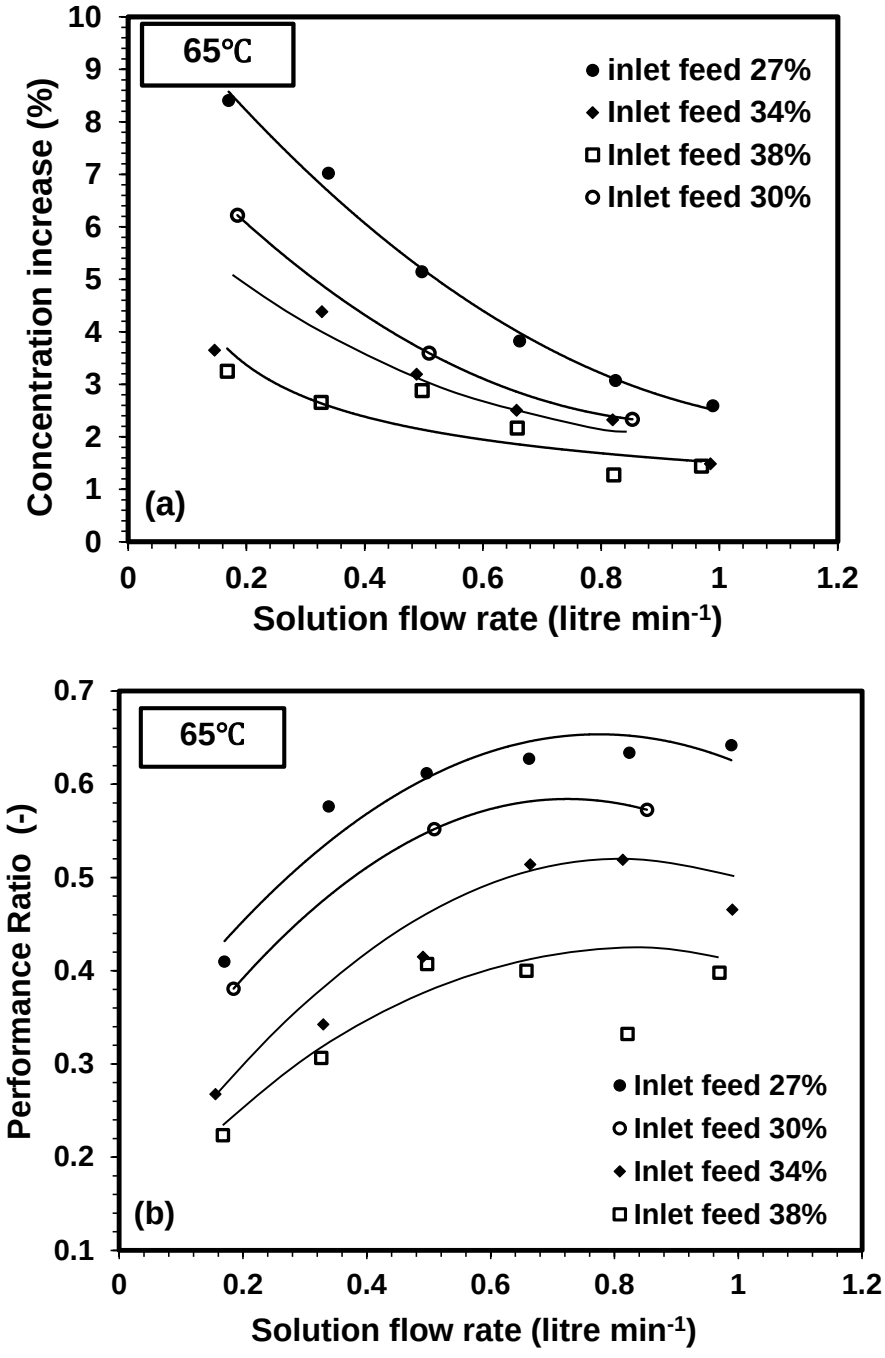
65℃
inlet feed 27%
Inlet feed 34%
Inlet feed 38%
Inlet feed 30%
(a)
Concentration increase (%)
Solution flow rate (litre min-1)
65℃
Inlet feed 27%
Inlet feed 30%
Inlet feed 34%
Inlet feed 38%
(b)
Performance Ratio (-)
Solution flow rate (litre min-1)

Figure 10

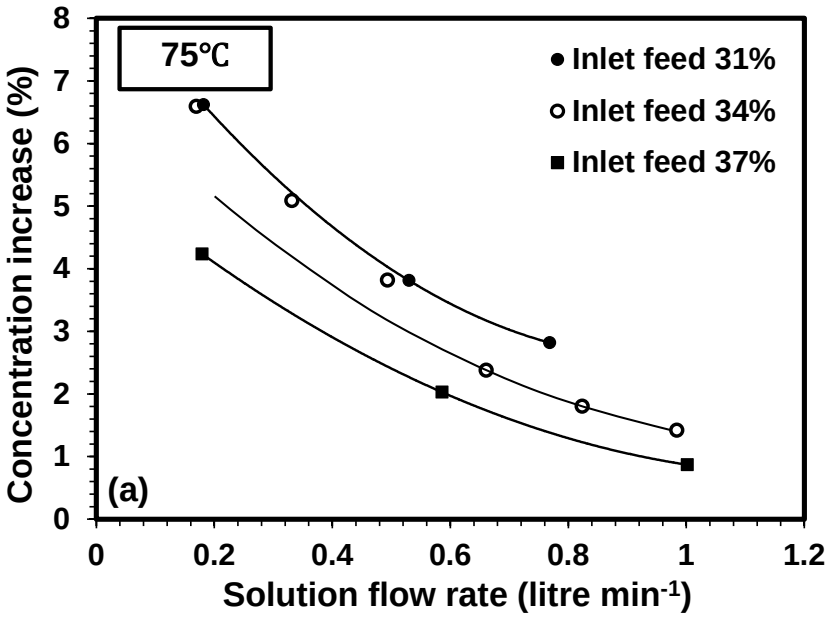
75℃
Inlet feed 31%
Inlet feed 34%
Inlet feed 37%
(a)
Concentration increase (%)
Solution flow rate (litre min-1)
0
1
2
3
4
5
6
7
8
0
0.2
0.4
0.6
0.8
1
1.2

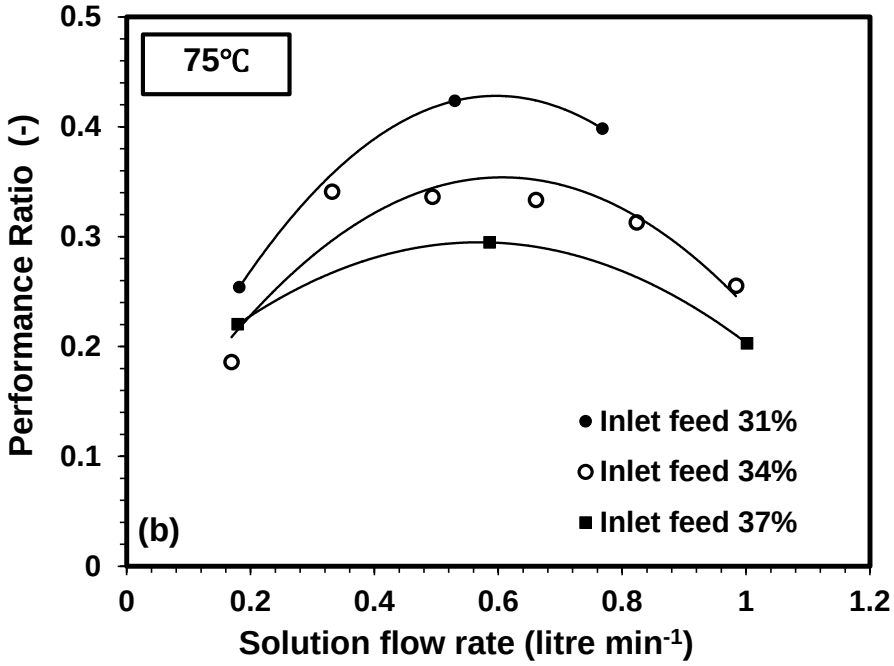
75℃
Inlet feed 31%
Inlet feed 34%
Inlet feed 37%
(b)
Performance Ratio (-)
Solution flow rate (litre min-1)
0
0.1
0.2
0.3
0.4
0.5
0
0.2
0.4
0.6
0.8
1
1.2

Figure 11

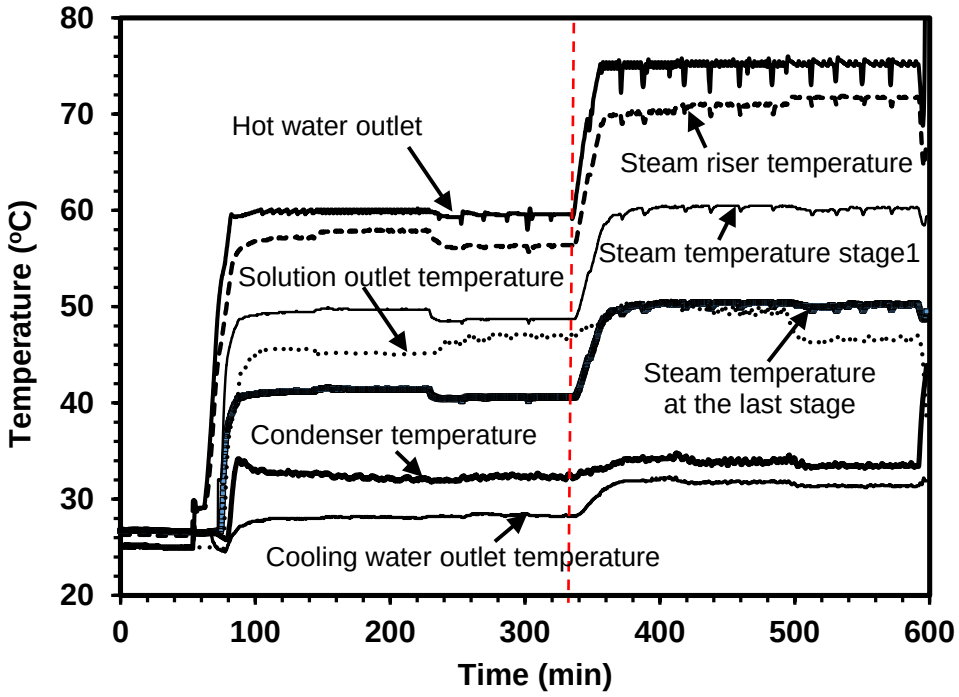
Temperature (°C)
Time (min)
Hot water outlet
Steam riser temperature
Steam temperature stage1
Solution outlet temperature
Steam temperature
at the last stage
Condenser temperature
Cooling water outlet temperature
80
70
60
50
40
30
20
0
100
200
300
400
500
600

Figure 12

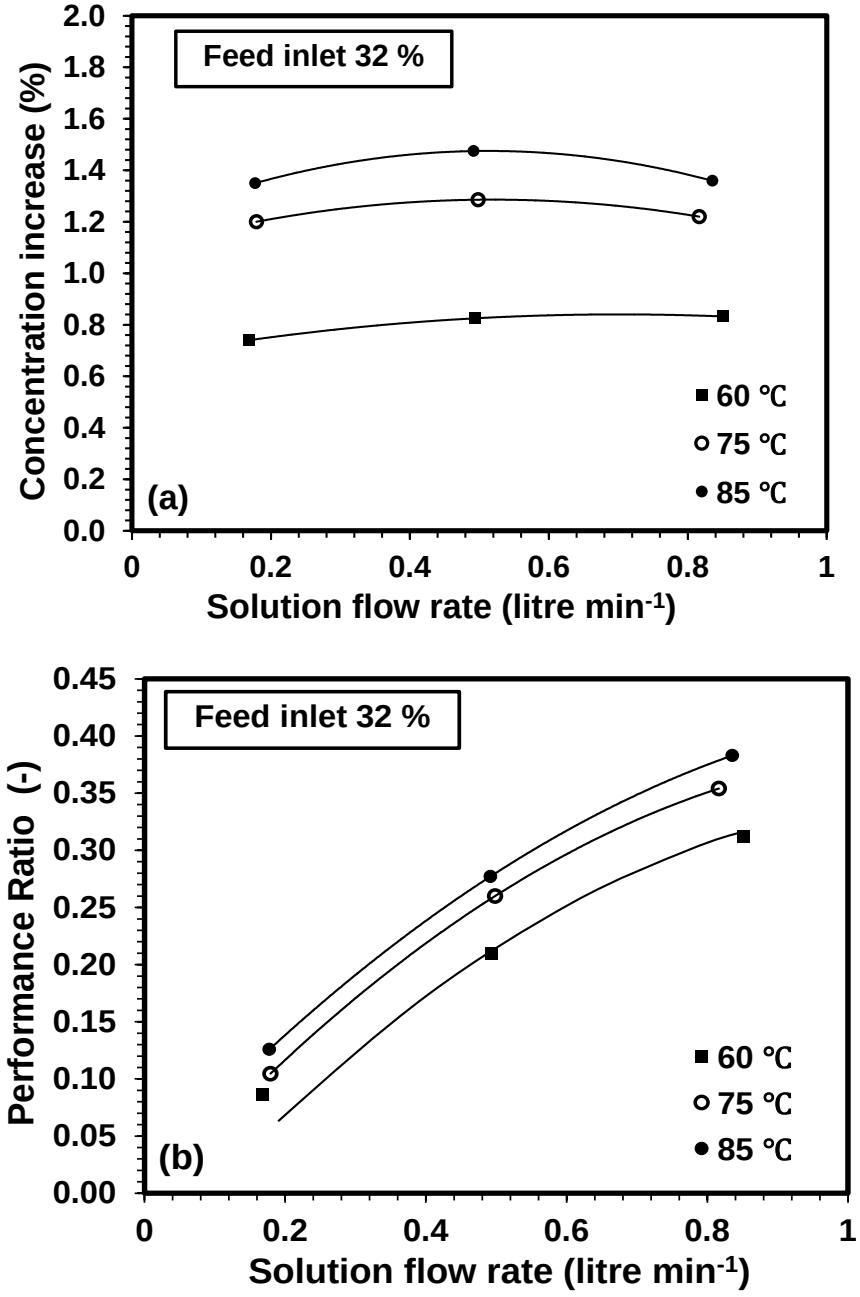
Feed inlet 32 %
Concentration increase (%)
Solution flow rate (litre min-1)
60 ℃
75 ℃
85 ℃
(a)
Feed inlet 32 %
Performance Ratio (-)
Solution flow rate (litre min-1)
60 ℃
75 ℃
85 ℃
(b)

Figure 13

List of Table

Table 1: Summary of various membrane distillations driven by low grade heat source.

Distillation type	Basic feature	Performances
Direct-contact-membrane distillation (DCMD) [23, 24]	• No external condenser is required. • Both hot and cold aqueous streams are in direct contact with membrane surface. • Requires relatively higher temperature.	• Performance ratio ranges from 0.2 to 0.9 depending on inlet feed temperatures. • Permeate flux varies from 20 kg/m^2h to 80 kg/m^2h.
Air-gap-membrane distillation (AGMD) [25, 26]	• Conductive heat loss through the membrane is greatly reduced. • Air gap increases the mass and heat transfer resistances. • Lower permeate flux.	• Energy efficiency ranges from 80% to 90% for a 3 mm air gap. • Minimum required temperature to drive the system is 65 ^oC. • Energy efficiency id reduced to 70% for the air gap of 1.5 mm
Sweep-gas-membrane distillation (SWMD) [27]	• Provides high mass transfer rate. • Relatively lower heat loss. • Complex heat recovery system.	• Permeate flux varies from 5 to 25 kg/m^2.h.
Vacuum membrane distillation (VMD) [17, 28]	• Reduce ab solute pressure in the downstream side of the membrane. • Overcomes the problem of air resistance to heat transfer. • Rapid water vapor transfer due to pressure gradients.	• Provides high performance ratio even at the feed inlet temperature of 50 ^oC. • High performance ratio for the inlet feed concentration of 8% or lower (sea water condition). • At higher concentration, the performance ratio drops significantly.